https://doi.org/10.5194/egusphere-2025-4446
Preprint. Discussion started: 18 September 2025

Spatio-temporal variability of greenhouse gas concentrations and fluxes in shallow coastal bays of the western Baltic Sea

Julika Zinke[1], Joakim P. Hansen[1], Martijn Hermans[1], Alexis Fonseca[1,2], Sofia A. Wikström[1], Linda Kumblad[1], Emil Rydin[1], Marc Geibel[1], Matthew E. Salter[1,3], and Christoph Humborg[1,3]

[1]Baltic Sea Centre, Stockholm University, Stockholm, Sweden
[2]Department of Ecology, Environment and Plant Sciences, Stockholm University, Stockholm, Sweden
[3]Department of Environmental Science, Stockholm University, Stockholm, Sweden

Corresponding author: Julika Zinke (julika.zinke@su.se)

Abstract. Coastal ecosystems play a crucial role in greenhouse gas (GHG) dynamics but are less studied than open oceans or terrestrial systems. This study measured concentrations of carbon dioxide (CO_2), methane (CH_4), and nitrous oxide (N_2O) in six shallow bays of the wider Stockholm Archipelago during spring (April) and fall (September–October) 2024 using cavity ring-down spectroscopy combined with a water equilibration system. We explored how GHG levels relate to bay characteristics and seawater properties, revealing significant seasonal variation concentrations. Surface water pCO_2 ranged from 225–1372 ppm, CH_4 from 3.6–580 nmol L^{-1}, and N_2O from 8–20.8 nmol L^{-1} with pCO_2 and CH_4 higher in fall and N_2O higher in spring. CH_4 concentrations below 250 nmol L^{-1} negatively correlated with N_2O, while higher CH_4 levels showed a positive correlation, indicating a shift in biogeochemical processes. All bays except the two most open ones (which acted as net sinks in spring) served as GHG sources at the time of sampling, with one anthropogenically degraded bay showing CH_4 emissions that surpassed CO_2 uptake. CO_2-equivalent fluxes ranged from -76.1 to 710.8 mg CO_2-eq m^{-2} d^{-2} (median: 56.9 mg CO_2-eq m^{-2} d^{-2}). These findings highlight the variability and complexity of coastal ecosystems and demonstrate the importance of high-resolution measurements for accurate up-scaling of fluxes from these dynamic environments.

1 Introduction

Coastal zones, particularly inshore habitats, are critical for understanding global GHG emissions since they are directly impacted by human activities at the land-ocean interface. Vegetated coastal ecosystems are highly productive and play an important role in carbon cycling (Al-Haj and Fulweiler, 2020) by capturing organic matter and taking up CO_2 from the atmosphere. However, this carbon sequestration is partly counterbalanced by the release of CH_4 and N_2O which have 100-year sustained global warming potentials 45 and 270 times greater than CO_2, respectively (Neubauer and Megonigal, 2015). Recent studies have shown that coastal habitats such as mangroves and salt marshes constitute significant sources of both CH_4 (Rosentreter et al., 2021a; Weber et al., 2019) and N_2O (Denman et al., 2007).

https://doi.org/10.5194/egusphere-2025-4446
Preprint. Discussion started: 18 September 2025

While mangroves, salt marshes, and seagrass ecosystems have been extensively studied, current estimates of coastal GHG emission budgets inadequately represent the diversity of coastal habitats, particularly shallow enclosed bays in brackish waters. Estimating GHG emissions in these diverse coastal environments is complex due to substantial spatial and temporal variability (Resplandy et al., 2024). Key influencing factors include vegetation type and density, sediment characteristics (organic content and porosity), salinity and corresponding sulfate availability, and eutrophication status (Rosentreter et al., 2021a; Al-Haj and Fulweiler, 2020). Additionally, GHG emissions show seasonal patterns driven by both biotic activity and abiotic factors such as oxygen availability, seawater temperature, wind speed and ice cover. This strong spatiotemporal variability makes scaling up GHG emissions from coastal areas using bottom-up approaches particularly challenging (Lundevall-Zara et al., 2021).

The biogeochemical processes underlying GHG production in coastal sediments are well understood. CO_2 is produced through respiration and decomposition of organic matter and can be consumed by photosynthesis of phytoplankton and vegetation. N_2O is generated as a by-product of denitrification or nitrification under suboxic and hypoxic conditions (Elkins et al., 1978; Codispoti, 2010) and has been shown to be controlled by the dissolved inorganic nitrogen (DIN) and oxygen availability (Murray et al., 2015). CH_4 is primarily produced via methanogenesis during organic matter degradation in anoxic sediments (Reeburgh, 2007; Amaral et al., 2021) and reaches the air-sea-interface through diffusive gas transfer and ebullition (Hermans et al., 2024), though during upward diffusion through the water column, dissolved CH_4 may be aerobically oxidized by methanotrophic bacteria, thereby limiting atmospheric flux.

Nevertheless, coastal eutrophication from increased nutrient input via river run-off and anthropogenic sources can destabilize the delicate equilibrium between methane production and oxidation (Żygadłowska et al., 2023; Venetz et al., 2024). Enhanced phytoplankton blooms and subsequent organic matter deposition on the seafloor lead to bottom-water oxygen depletion, which stimulates sediment methane generation while reducing CH_4 oxidation efficiency by methanotrophic microorganisms. While extensive oxygen depletion typically occurs in deeper coastal waters below the photic zone, it can also develop in shallower wave-protected areas where slow water exchange promotes organic matter accumulation (Wikström et al., 2025). The extensive archipelago regions of Sweden and Finland exemplify this phenomenon, containing numerous shallow, sheltered bays that accumulate substantial organic matter and function as potential carbon sinks (Gubri et al., 2025; Wikström et al., 2025). These shallow, enclosed bays cover approximately 142 km^2 across the Stockholm and Uppsala archipelagos, Åland islands, and southwestern Finnish archipelago (Gubri et al., 2025). Similar archipelago morphology, characterized by numerous embayments, is also found further north and south along the Swedish and Finnish coasts. Despite the Baltic Sea's well-documented eutrophication and its effects on coastal ecosystems, we currently lack sufficient knowledge to accurately upscale GHG emissions from these ecologically important shallow bay systems.

Recent advances in in situ measurement techniques, particularly cavity ring-down spectroscopy (CRDS), have enabled high-resolution, real-time monitoring of GHG concentrations in coastal waters (Rosentreter et al., 2021b; Roth et al., 2022). Using this technique, we conducted measurements of CH_4, CO_2, and N_2O in the surface waters of six shallow, sheltered, vegetated bays in the greater Stockholm Archipelago during two seasonal campaigns in April and September/ October 2024. Our aim was to characterize the spatial and temporal variability of surface water GHG concentrations in these underrepresented systems and to identify key environmental drivers. Our central hypothesis was that GHG concentrations and fluxes increase along a

https://doi.org/10.5194/egusphere-2025-4446
Preprint. Discussion started: 18 September 2025

eutrophication gradient and are influenced by geomorphological and physical factors such as water retention time and sediment composition. We further expected that the three GHGs would show distinct spatial patterns, with hotspots emerging in different niches within a bay, highlighting the need for detailed mapping to better estimate their overall climate feedback. To this end, we examined how GHG concentrations relate to bay characteristics including eutrophication indicators, vegetation cover, topographic openness, sediment properties, and water chemistry. These data provide critical insights into the functioning of shallow enclosed bays and contribute to more accurate scaling of coastal GHG emissions.

2 Methods

2.1 Study area

Continuous day-time measurements of CO_2, CH_4, and N_2O were conducted in the surface waters of six shallow bays in the Stockholm archipelago, Sweden (see Fig. 1). This region is characterized by a complex coastline with numerous shallow, sheltered bays that are variably separated from the surrounding Baltic Sea. The six study bays were selected to represent gradients in topographic openness and trophic status observed across the region, based on previous investigations of more than 20 shallow bays (e.g. Wikström et al., 2025; Gubri et al., 2025). Bay openness was quantified using the topographic openness index (Ea), calculated as $Ea = 100 \cdot \frac{At}{a}$, where At is the cross-sectional area of the bay opening and a is the total bay area. Three bays were classified as enclosed ($Ea \approx 0.01$), while three were semi-open ($Ea = 0.03 - 0.06$) (see Table 1). This metric is a reliable predictor of water retention time (Persson et al., 1994), sediment characteristics (Wikström et al., 2025) and biological communities (Munsterhjelm, 1997; Hansen et al., 2008; Snickars et al., 2009; Scheinin and Mattila, 2010), all of which can influence GHG cycling.

Within each openness category, we selected bays with varying eutrophication status based on historical total phosphorus and chlorophyll-a concentrations (see Table 1). Due to longer water retention times, enclosed bays naturally accumulated more nutrients and had higher chlorophyll-a concentrations than semi-open bays. All study bays were small (6 to 22 ha) and shallow (1.8–3.4 m, see Table 1), though semi-open bays were slightly deeper than enclosed ones.

https://doi.org/10.5194/egusphere-2025-4446
Preprint. Discussion started: 18 September 2025

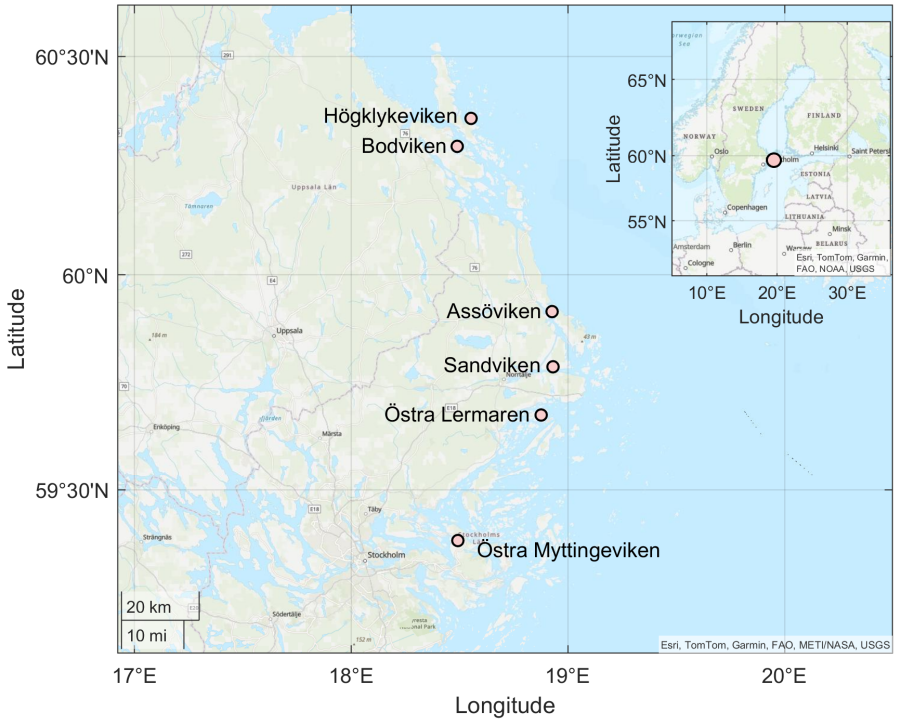

Figure 1. Location of the sampling bays in the wider Stockholm Archipelago in the Western Baltic Sea. Basemap data: ©Esri, TomTom, Garmin, FAO, MET/NASA/NOAA, USGS.

Table 1. Characteristics of the six study bays, including openness category, topographic openness index (Ea), physical dimensions, and phosphorus and chlorophyll concentrations in seawater. Mean and maximum total phosphorus (TP) and chlorophyll a (Chl a) concentrations represent historical data from 4 to 7 sampling occasions per year during 2020-2024 (spring through fall) and were used to characterize eutrophication status for bay selection. Bodviken (BV) was not sampled in 2020; Östra Lermaren (ÖL) not sampled in 2022-2023, the other bays were sampled all years.

Bay name	Bay category	Topographic openness (Ea)	Bay area (ha)	Maximum depth (m)	Mean (max) TP ($\mu g\,L^{-1}$)	Mean (max) Chl a ($\mu g\,L^{-1}$)
Högklykeviken (HV)	Enclosed	0.010	12	2.4	67 (114)	19 (58)
Bodviken (BV)	Enclosed	0.006	9	1.8	42 (73)	10 (26)
Östra Myttingeviken (ÖM)	Enclosed	0.013	6	2.5	39 (66)	8 (23)
Sandviken (SV)	Semi-open	0.026	22	3.4	41 (66)	8 (19)
Assöviken (AV)	Semi-open	0.032	17	3.2	37 (68)	7 (20)
Östra Lermaren (ÖL)	Semi-open	0.063	11	3.0	30 (49)	5 (10)

https://doi.org/10.5194/egusphere-2025-4446
Preprint. Discussion started: 18 September 2025

2.2 Continuous measurements of GHG concentrations

Measurements were conducted during midday in April and September/ October 2024 from a small boat. A cavity ring-down spectrometer (CRDS, model Picarro G2508, Picarro Inc., USA) coupled with a custom-built water equilibration gas analyzer system (WEGAS) was used to measure the concentrations of atmospheric and dissolved CO_2, CH_4 and N_2O.

2.2.1 The WEGAS system

The WEGAS system is described in detail in Humborg et al. (2019). Briefly, seawater from just below the surface (at approximately 30 cm depth) was continuously passed through a water handling system consisting of a thermosalinograph (SBE45 MicroTSG, Seabird Scientific, US) measuring seawater temperature, salinity, and conductivity; a flowmeter maintaining stable flow at $\sim 3\,\mathrm{L\,min^{-1}}$; and a showerhead equilibrator (RAD-AQUA, Durridge, US). After the seawater was equilibrated with a flow of ambient air, the air stream was passed through a custom-built cryocooler that cooled the gas to a dew point of 4°C to reduce excess humidity before analysis by the CRDS. A gas handling system controlled airflow switching between ambient air measurements and equilibrator measurements. Each sampling cycle consisted of 5 minutes of ambient air followed by 40 minutes of equilibrator air, with cycles repeated until horizontal profiling of each bay was completed. Transition periods between ambient and equilibrator air were excluded from analysis.

2.2.2 Gas concentration calculations

Partial pressures (ppm) of CH_4 and N_2O were converted to molar concentrations using Henry's law (equation 1), assuming full equilibration in the equilibrator at ambient pressure:

$$C = p \times K_H \tag{1}$$

where C is concentration ($\mathrm{mol\,L^{-1}}$), p is the partial pressure (atm=10^6 ppm), and K_H is the temperature-corrected Henry's law constant:

$$K_H = K_H^* \times \exp\left(\frac{-\Delta_{\mathrm{sol}}\mathrm{H}}{\mathrm{R}} \times \left(\frac{1}{\mathrm{T_K}} - \frac{1}{298.15\ \mathrm{K}}\right)\right). \tag{2}$$

where K_H^* is the Henry's law constant at reference temperature (298.15 K), $\Delta_{\mathrm{sol}}H$ is the enthalpy of dissolution, R is the gas constant and T_K is water temperature in Kelvin. Constants were obtained from Sander (2015).

Gas solubilities were calculated using the Bunsen solubility coefficient:

$$\beta = \exp\left(\mathrm{A_1} + \mathrm{A_2}\left(\frac{100}{\mathrm{T}}\right) + \mathrm{A_3}\ \ln\left(\frac{\mathrm{T}}{100}\right) + \mathrm{S}\left(\mathrm{B_1} + \mathrm{B_2}\left(\frac{\mathrm{T}}{100}\right) + \mathrm{B_3}\left(\frac{\mathrm{T}}{100}\right)^2\right)\right) \tag{3}$$

https://doi.org/10.5194/egusphere-2025-4446
Preprint. Discussion started: 18 September 2025

where β is the dimensionless Bunsen coefficient, A_1–A_3 and B_1–B_3 are gas-specific constants from Wiesenburg and Guinasso Jr (1979), T is temperature (K), and S is salinity ($\mathrm{g\,kg^{-1}}$). For N_2O, $K_0 = \beta$. For CH_4 (ideal gas behavior), $K_0 = \beta(R \times 273.15\ \mathrm{K})$.

2.2.3 Air-sea flux calculations

Air-sea fluxes were estimated using:

$$F = k \times K_0 \times (pX_{\mathrm{seawater}} - pX_{\mathrm{air}}). \tag{4}$$

where F is flux, k is gas transfer velocity ($\mathrm{m\ s^{-1}}$), K_0 is solubility, and pX represents partial pressures in seawater and air. The gas transfer velocity was calculated following Cole and Caraco (1998) which is representative for lake environments:

$$k = (2.07 + 0.251 \times U_{10}^{1.7}) \times (\frac{Sc}{600})^{-0.5}. \tag{5}$$

where U_{10} is wind speed and Sc is the Schmidt number. Schmidt numbers for brackish Baltic Sea conditions were interpolated between freshwater and seawater values (Wanninkhof, 2014):

$$Sc_{\text{this study}} = (Sc_{\mathrm{seawater}} - Sc_{\mathrm{freshwater}}) \times \frac{S}{35} + Sc_{\mathrm{freshwater}}\ . \tag{6}$$

Wind speed was not measured during this study. Given the sheltered nature of all bays and absence of white-capping (typically occurring at $U \geq 4\ \mathrm{m\ s^{-1}}$), we used a constant wind speed of $2\ \mathrm{m\ s^{-1}}$ for all flux calculations.

2.2.4 CO_2-equivalent fluxes

To derive CO_2-equivalent fluxes, calculated fluxes ($\mu\mathrm{mol\,m^{-2}day^{-1}}$) were converted to mass units ($\mathrm{mg\,m^{-2}\,day^{-1}}$) using respective molar masses, then multiplied by 100-year sustained global warming potentials of 45 for CH_4 and 270 for N_2O (Neubauer and Megonigal, 2015).

2.3 Collection and analysis of seawater and sediment samples

2.3.1 Water sample collection and laboratory analysis

Surface water samples (0–1 m depth) were collected from the centre of each bay and kept cool until analysis at the certified Erken laboratory, Uppsala University (ISO/IEC 17025). Dissolved concentrations of nitrite-N and nitrate-N (NO_2-N + NO_3-N), ammonium-N (NH_4-N) and phosphate-P (PO_4-P) were determined colorimetrically using an AutoAnalyzer 3 (SEAL Analytical, US) or a U-2910 analyser (Hitachi, Japan). Total nitrogen (TN) and phosphorus (TP) concentrations were determined as NO_3-N and PO_4-P after persulfate digestion.

https://doi.org/10.5194/egusphere-2025-4446
Preprint. Discussion started: 18 September 2025

Chlorophyll a (Chl a) was determined spectrophotometrically after acetone extraction. Total organic carbon (TOC) was analyzed using a 680°C combustion catalytic oxidation method with a TOC-L analyser (Shimadzu, Japan). Organic content was estimated as loss on ignition (LOI) after combustion at 550°C. Turbidity was measured as Formazin Nephelometric Units (FNU) using a 2100 P ISO turbidity meter (Hach, CO, USA).

2.3.2 In-situ water measurements

Temperature, salinity and dissolved oxygen were measured using a WTW Multi 3420 probe (Xylem, US), and pH was measured with a YSI Pro10 pH meter (Xylem, US). All measurements were taken in the centre of each bay, adjacent to the water sampling location.

2.3.3 Vegetation surveys

Aquatic vegetation cover was visually estimated by a free-diver in August, a few weeks prior to the September GHG measurements. For two bays (Högklykeviken and Bodviken), vegetation cover was also estimated in May, a few weeks after the April GHG measurements. For the other two bays with GHG measurements in May (Assöviken and Sandviken), we retrieved May vegetation data from a previously conduced survey (in 2022). The interannual variation in total vegetation cover is rather small in these bays. Survey plots consisting of 7–13 circular areas (5 m radius, ~ 80 m^2) were distributed evenly from the bay opening to the innermost areas. Plots were randomly allocated within subareas along a distance-from-opening gradient, excluding nearshore areas with < 0.5 m water depth. Within each plot, percentage cover of individual taxa was recorded, and total cover of all macroscopic autotrophs (including filamentous algae and cyanobactera) was estimated. For this study, we used two vegetation indicators: (1) total vegetation cover and (2) cumulative cover of all rooted vegetation (sum of all rooted taxa cover).

2.3.4 Sediment sampling and analysis

Sediment cores were collected using a gravity corer (63 mm inner diameter) and sectioned on-site immediately upon return to land. Cores were sliced at the following depth intervals: 0–1 cm, 1–3 cm, 3–5 cm, 5–7 cm, 7–9 cm, 9–11 cm, 11–13 cm, 13–15 cm, 20–22 cm and 28–30 cm. Sediment samples from each interval were homogenized in sterile containers and transferred to pre-weighed polypropylene vials for analysis. Samples were freeze-dried and pulverized to fine powder. Porosity was calculated from weight loss after freeze-drying, assuming a sediment dry density of 2.65 g cm^{-3} (Burdige, 2020). Sediment water content was determined after freeze-drying, and organic content was determined by loss on ignition (LOI) at 550°C for 2 h. Organic carbon (C_{org}) and nitrogen (N_{org}) content were determined using an Elemental Combustion System (ECS 4010, Costech Analytical Technologies Inc, US). For this study, we used only data from the uppermost sediment layer (0–1 cm) as it represents the most biogeochemically active zone and is most relevant to surface water GHG dynamics.

https://doi.org/10.5194/egusphere-2025-4446
Preprint. Discussion started: 18 September 2025

3 Results and Discussion

3.1 Spatio-temporal variability of GHG across shallow bays

Surface water concentrations of CH_4, pCO_2, and N_2O exhibited substantial spatial and temporal variability across the six study bays, between seasons, and between areas inside and outside the bays (see Fig. 2 and Fig. A1-A6 in the appendix). Statistical analysis using Kruskal-Wallis tests (based on 10% of the data to avoid interdependence between neighbouring measurement points) confirmed significant differences in GHG concentrations between bays (see Table A1 in the appendix). Calculating post-hoc Bonferroni corrected p-values allowed us to discern which bays differed from each other (see Table A2). A Wilcoxon rank-sum test further showed significant differences between inside and outside bay areas for all gases (see Table A3).

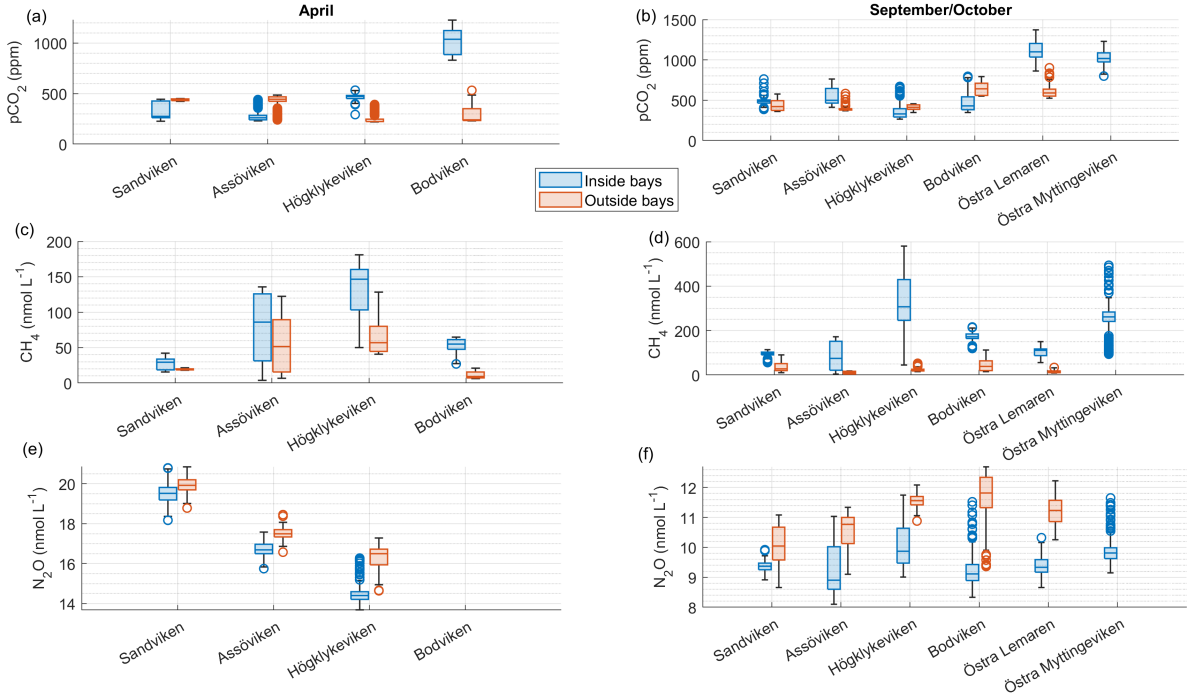

Figure 2. Spatial variation of surface water concentrations of (a-b) CO_2, (c-d) CH_4 and (e-f) N_2O across six shallow bays in April and September/October 2024. Box plots show median, quartiles, outliers and range for measurements inside (blue) and outside (red) each bay. N_2O data were not available for Bodviken, and no outside measurements were obtained for Östra Myttingeviken in October.

3.1.1 CO_2 concentrations and patterns

CO_2 was generally slightly supersaturated in surface waters, with concentrations differing significantly between bays (see Table 2 and A1). The highest concentrations were observed in Bodviken during April (mean 1022±121.6 ppm) and in Östra Lermaren and Östra Myttingeviken during October (mean 1108±117.7 ppm and 1033±83.1 ppm, respectively). These bays

https://doi.org/10.5194/egusphere-2025-4446
Preprint. Discussion started: 18 September 2025

showed significantly higher CO_2 concentrations inside compared to outside areas (see Table A2). Overall, no consistent patterns emerged between bay openness categories or between inside versus outside areas across all bays and seasons, indicating high spatial and temporal variability in CO_2 dynamics.

The bays with elevated CO_2 concentrations shared several characteristics: extensive vegetation cover, very high sediment organic carbon content and lower eutrophication status compared to other study sites (see Tables 3 and 4). While it might seem counter-intuitive that the least eutrophied and most vegetated bays act as hotspots for CO_2 emissions, this might be due to high allochthonous, terrestrial input and autochthonous input from decaying plant matter. This pattern aligns with other coastal studies documenting seasonal CO_2 hotspots in areas with elevated organic matter input due to remineralization processes (Amaral et al., 2021; Asmala and Scheinin, 2024).

The CO_2 concentrations observed in our study bays were at the high end of or exceeded those reported from more open archipelago areas in the Eastern Baltic Sea. Previous studies reported: 750 ppm (Humborg et al., 2019), 4.5-13,100 ppm (Asmala and Scheinin, 2024), and 92-697 ppm (Brunberg et al., 2025). Notably, maximum values in our study compared well with the mean concentrations of 1288 ppm reported from Swedish lakes (Humborg et al., 2010). This similarly suggests that these transitional environments between lakes and fully marine environments may share characteristics with lake systems regarding GHG emissions.

These findings indicate that while shallow bays often accumulate organic matter and are significant reservoirs of carbon and nutrients accumulated from surrounding areas (Gubri et al., 2025; Wikström et al., 2025), they may simultaneously represent an overlooked coastal CO_2 source to the atmosphere, particularly during periods of low pelagic production. However, our measurements represent only snapshots from two seasons. More extensive, long-term monitoring is required to identify the environmental parameters that drive these systems to function as CO_2 sources or sinks across different temporal scales.

3.1.2 CH_4 concentrations and patterns

CH_4 was strongly supersaturated in all study bays and significantly higher inside bays compared to open water (as shown using a Wilcoxon rank-sum test, see Table A2 in the appendix). Concentrations were generally higher in fall compared to spring (see Fig. 2c,d and Table 2), likely reflecting enhanced organic matter degradation and increased activity of methanogenic archaea in anoxic sediments (Conrad, 2009). The highest concentrations were recorded in Högklykeviken, reaching 181 nmol L^{-1} in April and 580 nmol L^{-1} in September. Östra Myttingeviken also showed elevated levels up to 494 nmol L^{-1}. Both are enclosed bays, with Högklykeviken representing a more degraded system that has shifted from benthic vegetation dominance to plankton dominance.

Methane production occurs primarily through methanogenic archaea in oxygen-depleted sediments (Schubert and Wehrli, 2019). In enclosed bays with narrow openings, limited water exchange minimizes sediment disturbance by waves and currents, allowing organic matter to accumulate and creating conditions conducive to elevated CH_4 production. Recent studies have shown that such shallow, sheltered bays are significant organic carbon reservoirs, with higher accumulation correlated with vegetation cover, coastal morphology, and landscape characteristics (Wikström et al., 2025).

https://doi.org/10.5194/egusphere-2025-4446
Preprint. Discussion started: 18 September 2025

Our observations align with previous research showing that sediment porosity and organic content positively influence CH_4 concentrations (Lundevall-Zara et al., 2021; Roth et al., 2022), while rooted vegetation can negatively impact CH_4 concentrations, likely because plant roots transport oxygen to sediments, suppressing methanogenesis while enhancing methane oxidation by aerobic methanotrophs.

In April, higher CH_4 concentrations were associated with warmer seawater temperature, consistent with previous studies (e.g., Lundevall-Zara et al., 2021; Roth et al., 2022). Elevated temperatures accelerate microbial metabolic rates and enzymatic activities boosting methanogenic rates (Yvon-Durocher et al., 2014; Reay et al., 2018). Warmer seawater temperatures also decrease CH_4 solubility and enhance stratification, reducing mixing and potentially increasing concentrations.

Higher CH_4 concentrations were observed in bays with lower salinity during fall, consistent with previous research (e.g., Lundevall-Zara et al., 2021; Roth et al., 2022). Salinity inhibits CH_4 production through multiple mechanisms, including increased sulfate availability that favors sulfate-reducing bacteria over methanogens (Camacho et al., 2017; Poffenbarger et al., 2011). The WEGAS system measures CH_4 from both benthic diffusion and bubble dissolution. Without isotopic data, distinguishing between diffusive transport or ebullition events is not possible.

Our measured concentrations (up to 580 nmol L^{-1}) are comparable to previous studies in the Baltic Sea region. Studies around Askö reported 6–460 nmol L^{-1} (Roth et al., 2022) and 26-6596 nmol L^{-1} (Lundevall-Zara et al., 2021), while Tvärminne Archipelago studies reported ranges of 12.8–114 nmol L^{-1} (Brunberg et al., 2025), 44 nmol L^{-1} (Humborg et al., 2019), 130-665 nmol L^{-1} (Myllykangas et al., 2020), and 0-6767 nmol L^{-1} (Asmala and Scheinin, 2024). The consistent observation of high spatial variability and local CH_4 hotspots across these studies underscores the need for high-resolution sampling to accurately characterize GHG dynamics in shallow coastal ecosystems.

3.1.3 N_2O concentrations and patterns

N_2O concentrations showed pronounced seasonal variation, with higher values in spring (13.7–20.8 nmol L^{-1}) than in fall (8–11.75 nmol L^{-1}). Most bays were slightly subsaturated or close to saturation, except for Sandviken and Assöviken in April, which exhibited supersaturation. A clear spatial pattern emerged in April, with higher concentrations in open bays compared to enclosed bays (see Fig. 2e), while no such trend was apparent in September data. In addition, N_2O concentrations were generally higher outside bays than inside, contrasting with the patterns observed for CH_4.

Higher N_2O concentrations were associated with lower seawater temperatures in April. This relationship is likely driven by two key factors: (1) increased N_2O solubility at lower temperatures, and (2) the temperature sensitivity of denitrification enzymes. Specifically, cold temperatures inhibit the nosZ enzyme that encodes nitrous oxide reductase, a crucial enzyme in the denitrification process responsible for reducing N_2O to N_2. Contrary to findings reported by Murray et al. (2015), we could not observe a correlation between the concentrations of NO_2+NO_3 and N_2O across the bays.

The consistently higher N_2O concentrations outside the bays can be explained by higher flow rates and coarser sediments (sand, gravel, stones) that promote denitrification processes. Lower concentrations inside bays are likely the result of reduced flow rates and accumulation of fine organic matter, creating different biogeochemical conditions. N_2O production in these sys-

https://doi.org/10.5194/egusphere-2025-4446
Preprint. Discussion started: 18 September 2025

tems results from nitrification and denitrification processes mediated by distinct microbial communities. Ammonia-oxidizing bacteria and archaea (AOB and AOA) initiate nitrification, producing nitrite and nitrate, which are then reduced by denitrifying microbes under low-oxygen conditions potentially producing N_2O as an intermediate product (Stein, 2020).

Few studies have simultaneously measured CO_2, CH_4 and N_2O in shallow Baltic Sea bays. Our results are similar to those of Brunberg et al. (2025), who reported similar seasonal patterns in the Tvärminne Archipelago: higher N_2O concentrations up to 20.2 nmol L^{-1} in April compared to 8-12 nmol L^{-1} in August and October. They suggested that spring N_2O peaks relate to sedimentation of the phytoplankton spring bloom and associated nitrification/denitrification processes. Similarly, studies from the southern Baltic Sea (Ma et al., 2019; Cheung et al., 2025) observed pronounced seasonal patters with higher concentrations in winter and spring and low concentrations in fall when anoxic and hypoxic conditions predominate.

https://doi.org/10.5194/egusphere-2025-4446
Preprint. Discussion started: 18 September 2025

Table 2. Mean concentrations, ranges, and saturation percentages of CH_4, CO_2, and N_2O inside and outside of six bays in April and September.

Bay Name	Month	Location	CH_4 range ($nmol\,L^{-1}$)	CH_4 mean ($nmol\,L^{-1}$)	CH_4 sat. (%)	pCO_2 range (ppm)	pCO_2 mean (ppm)	CO_2 sat. (%)	N_2O range ($nmol\,L^{-1}$)	N_2O mean ($nmol\,L^{-1}$)	N_2O sat. (%)
Sandviken	April	Inside	15.3–42.3	27.6±7.9	546.2±155.9	225.1–443.8	321.7±78.1	149.8 ± 36.4	18.2–20.8	19.5±0.5	116.6±2.7
		Outside	17.9–21.4	19.2±0.97	380.1 ± 19.3	423.6–449.15	437.7±8.6	203.8±3.98	18.8–20.9	19.9±0.4	119.2±2.15
	September	Inside	55.9–113.5	94.7±13.6	2367.9±345.6	386.7–762.7	483.6±48.6	189.3±18.3	8.9–9.9	9.4±0.17	89.9±1.7
		Outside	9.8–90.3	38.2±25.3	1253.9±739.5	361.3–576.3	433.1±60.3	166.9±24.3	8.7–11.1	10.1±0.6	98.6±5.98
Assöviken	April	Inside	3.7–135.9	78.6±45.0	850.9±489.1	227.9–440.4	321.7±78.1	118±21	15.7–17.6	16.7±0.4	106±1.8
		Outside	6.6–122.5	57.5±36.6	588.8± 380.5	239.7–486.7	437.7±8.5	185.3±33.15	16.5–18.5	17.5±0.3	103.55±2.4
	September	Inside	3.9–171.5	85.9±59.8	2925.6±1245.2	413.6–763.8	483.6±48.6	211.8±42.1	8.1–11.0	9.3±0.9	86.5±5.3
		Outside	3.6–18.3	10.9±5.6	446.9±262.5	369.3–583.2	433.1±60.3	154.6±14.7	9.1–11.3	10.6±0.5	104.2±2.1
Högklykeviken	April	Inside	49.9–180.9	133.8±35.5	1425.9±374	292.4–533.3	465.3±28.5	202±12.2	13.7–16.3	14.5±0.6	90±1.4
		Outside	40.6–180.9	66.7±27.6	674± 270.1	218.8–391.5	252.1±53.5	111.2±22.9	14.6–17.3	16.3±0.6	95.7±1.8
	September	Inside	44.5–580.3	327.7±131.1	8267.7±3330.9	267.0–671.2	363.3±97.4	141.8±38.4	9.0–11.8	10.0±0.7	95.4±6.1
		Outside	14.7–52.5	23.3±8.6	572.6±214.4	346.5–456.4	413.4±31.2	163.1±12.5	10.9–12.1	11.6±0.2	105.8±1.6
Bodviken	April	Inside	26.9–64.8	52.1±10.9	564.9±118.5	829.7–1226.1	1022.5±121.6	441.5±52.2	-	-	-
		Outside	6.3–20.7	11.1±4.5	113.3± 47.6	230.3–532.2	285.9±72.8	126±31.2	-	-	-
	September	Inside	119.4–215.9	172.9±17.1	4304.4±448.0	347.7–796.4	469.7±109.4	184.4±43.9	8.3–11.5	9.3±0.6	86.4±4.3
		Outside	15.1–112.4	43.5±24.2	1084.6±636.3	551.4–791.6	638.5±70.6	258.3±31.3	9.4–12.7	11.7±0.8	104.7±3.6
Östra Lermaren	October	Inside	56.1–149.3	106.4±22.9	2540.2±553.7	861.9–1371.8	1108.2±117.7	443.6±47.3	8.7–10.3	9.4±0.3	82.1±2.4
		Outside	9.2–33.7	15.2±6.8	360.2±159.6	523.8–902.3	28.1±3.9	245.8±34.4	10.3–12.2	11.2±0.45	97.9±4.9
Östra Myttingeviken	October	Inside	93.6–493.9	225.6±76.7	5604±1898.3	799.6–1231.3	1033.6±83.1	422.9±32.5	9,1–11.65	9.9±0.4	81.4±4.4

https://doi.org/10.5194/egusphere-2025-4446
Preprint. Discussion started: 18 September 2025

Table 3. Seawater properties in the different bays in April and September, including seawater temperature (T_{SW}), salinity (S), dissolved oxygen at seafloor, chlorophyll-a (Chl-a) concentration, turbidity, pH, total organic carbon (TOC), loss of ignition (LOI) as well as dissolved concentrations of total phosphorus (TP), phosphate (PO_4), total nitrogen (TN), nitrite and nitrate (NO_2+NO_3).

Bay abbrev.	Month	T_{SW} (°C)	S (g kg^{-1})	Dissolved oxygen %	Chl-a (μg L^{-1})	Turbidity (FNU)	pH	TOC (μg L^{-1})	LOI (mg L^{-1})	TP (μg L^{-1})	PO_4 (μg L^{-1})	TN (μg L^{-1})	NO_2+NO_3 (μg L^{-1})
SV	April	3.8	4.5	109	11.1	2.3	7.94	6.9	2.3	25.2	1.94	397	1.37
	Sept.	15	5.5	96	6.3	4.3	7.94	6.6	8.0	44.67	5.4	539.4	1.44
AV	April	3.6	4.8	102	9.5	1.2	7.7	6.1	1.6	29.8	4.3	417	27.2
	Sept.	15.1	5.6	85	13.5	3.1	7.7	7.7	4.2	46.7	0	719.6	1.8
HV	April	3.3	4.1	104	6.9	1.7	7.8	7.4	3.4	34.9	0.85	464	1.85
	Sept.	14.9	5.4	91	13.6	3.2	7.8	10.8	7.5	58.6	0.4	944.15	1.98
BV	April	6.4	3.2	96	9.3	4.2	7.7	11.85	2.4	35.7	3.95	644	2.76
	Sept.	13.3	5.3	76	22.0	2.3	7.8	8.85	7	60.6	0.8	799.7	1
ÖL	Oct.	11.4	5.6	NA	4.7	1.36	7.56	6.1	2.4	23.5	0	530.2	1.98
ÖM	Oct.	9.6	4.5	59	4.1	0.8	7.4	7.0	2.1	26.1	2.7	495.2	0.46

Table 4. Sediment and vegetation properties in the different bays in April and September including the total cover of aquatic vegetation, cumulative cover of rooted vegetation, organic carbon (OC_{sed}) and organic nitrogen ON_{sed} in the sediment and sediment porosity.

Bay abbrev.	Month	Total vegetation %	Rooted vegetation %	OC_{sed} (0-1 cm) (wt%)	ON_{sed} (0-1 cm) (wt%)	Porosity (0-1 cm)
SV	April	12	7	-	-	-
	Sept.	32	23	6.73	0.9	0.94
AV	April	30	4	-	-	-
	Sept.	54	27	8.75	1.07	0.93
HV	April	29	3	-	-	-
	Sept.	32	20	13.3	1.7	0.97
BV	April	79	18	-	-	-
	Sept.	96	60	10.2	1.2	0.96
ÖL	Oct.	77	63	22.3	2.4	0.98
ÖM	Oct.	65	46	28.6	4.0	0.98

https://doi.org/10.5194/egusphere-2025-4446
Preprint. Discussion started: 18 September 2025

3.1.4 Correlation between N_2O and CH_4

Negative correlations between N_2O and CH_4 were observed across different bays and seasons (see Fig. 3). Similar patterns were observed in measurements conducted around Askö in September 2020 and March 2021 (see Fig. 3a, unpublished data collected by Florian Roth, measured using the same sampling setup).

This negative correlation can be likely explained by the spatial distribution of the gases. N_2O concentrations were generally highest outside the bays and in the channels that connect to the open sea, where the flow velocities are higher and the coarser substrates (sand, gravel, stones) dominate. This aligns with previous studies (as reviewed in Murray et al., 2015), who observed that high-energy environments with turbulent regimes and coarser sediment types are N_2O hot spots. In contrast, CH_4 was highest inside the bays, where sedimentary organic matter accumulates in fine muddy sediments. This creates a gradient where decreasing flow velocity from bay openings toward inner areas corresponds with decreasing N_2O and increasing CH_4

However, in Högklykeviken and Östra Myttingeviken, the bays with the highest fall CH_4 concentrations, we observed an interesting shift from negative correlations at CH_4 concentrations $<$250 nmol L^{-1} to positive correlations at CH_4 concentrations $>$250 nmol L^{-1}. This threshold behaviour suggests that different biogeochemical processes dominate at high versus low CH_4 concentrations, which is indicative of the complex redox dynamics of these systems. Importantly, in these two bays, high N_2O concentrations were also measured above shallow, muddy areas furthest into the bays, contradicting the general spatial pattern.

The different spatial distributions of CH_4 and N_2O are most likely due to their different optimal oxygen conditions: CH_4 production occurs mainly in anoxic regions, while N_2O production is maximal at suboxic levels near oxygen minimum zones where denitrification dominates (Naqvi et al., 2010; Ji et al., 2015, 2018; Foster and Fulweiler, 2016; Barnes and Upstill-Goddard, 2018; Tang et al., 2022). Our measured dissolved oxygen levels indicate generally oxic conditions in both Högklykeviken ($O_{2,\mathrm{dissolved}} = 8.3\,\mathrm{mg\,L^{-1}} \approx 91\%$) and Östra Myttingeviken ($O_{2,\mathrm{dissolved}} = 5.6\,\mathrm{mg\,L^{-1}} \approx 59\%$), though minimum levels reached 71% and 23% saturation, respectively. Since measurements were taken in the center of the bays (Table 3 and also marked location in the maps, Fig. A1-A6) there might have been local hypoxia or anoxia where CH_4 peaks were observed. The local peaks in N_2O might be due to periodic O_2 entrainment events where suboxia occurs close enough to the sea surface to allow respiration (Codispoti, 2010). Alternatively, sediment disturbance from the research vessel in very shallow areas could explain these anomalous patterns.

In Högklykeviken, an additional factor may have influenced these relationships. As part of a coastal restoration project, an aluminum-based geoengineering treatment was conducted on 13 May 2024 in the area where both CH_4 and N_2O exhibited high concentrations and positive correlations. This treatment involved injecting an aluminum solution into the sediment to increase the phosphorus retention and reduce eutrophication. Previous research has suggested that aluminium can decrease organic matter remineralization, possibly slowing methane production (Reitzel et al., 2006; Zhou et al., 2018; Scalize et al., 2021), while Zhou et al. (2018) reported enhanced nitrogen fixation in the presence of aluminum. Whether this sediment disturbance altered microbial communities and affected GHG emissions requires further investigation that is beyond the scope of this study.

https://doi.org/10.5194/egusphere-2025-4446
Preprint. Discussion started: 18 September 2025

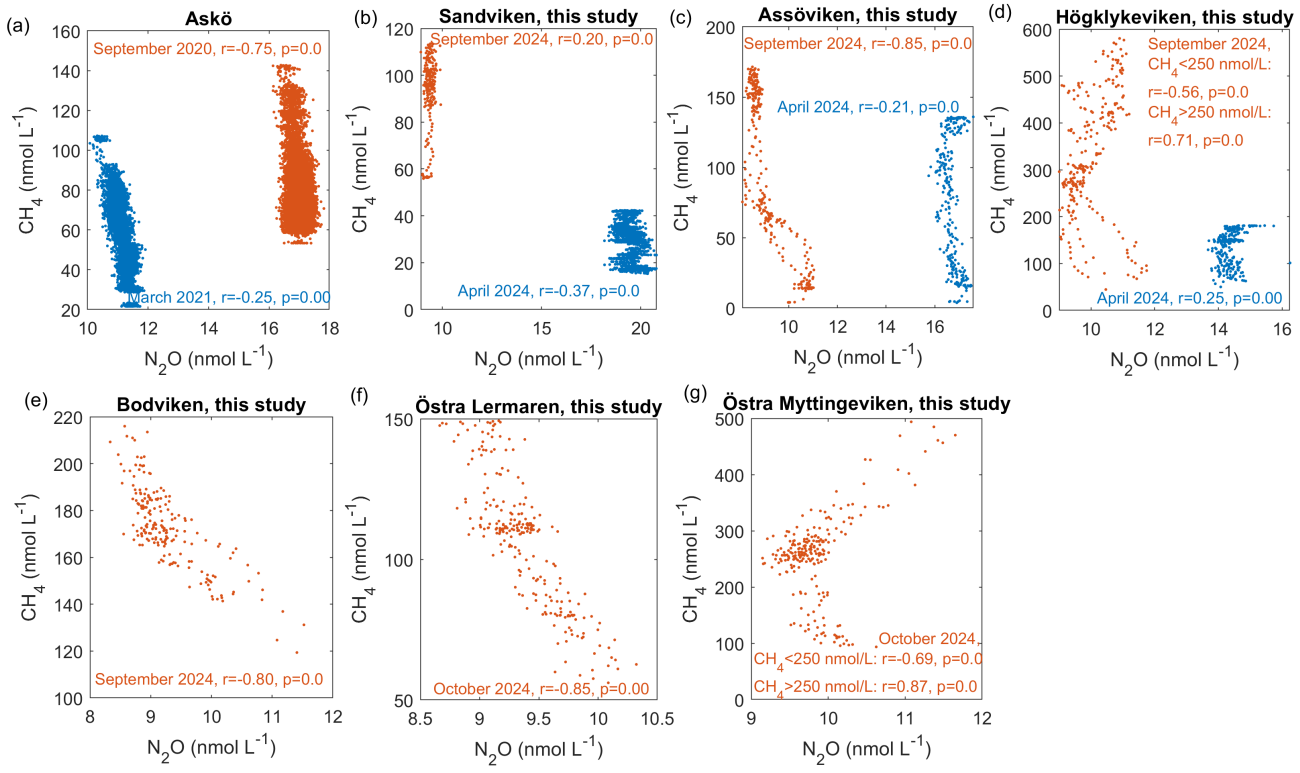

Figure 3. Correlations between N_2O and CH_4 across different bays, seasons and studies, also including data from Askö (data collected by Florian Roth).

3.2 Flux estimates from shallow bays

To determine whether these bays acted as net sources or sinks of GHG, air-sea fluxes were calculated using the methods described in section 2.2. Individual gas flux densities had high variability between bays and seasons, similar to the complex spatial and temporal patterns observed in the surface water concentrations.

CO_2 flux densities were highly variable ranging from -68 to 272 mg CO_2 m^{-2} d^{-1} in spring and -29 to 303 mg CO_2 m^{-2} d^{-1} in fall. The negative values indicate CO_2 uptake (sinks), while positive values are representative of emissions to the atmosphere (sources).

CH_4 flux densities were generally positive across all bays and seasons and ranged from 0.05 to 1.1 mg CH_4 m^{-2} d^{-1}, suggesting that all study sites acted as CH_4 sources. These estimates are similar to those reported for similar habitats by Roth et al. (2022) and fall within a similar range of global estimates for tidal systems, lagoons, and fjords (Rosentreter et al., 2023).

https://doi.org/10.5194/egusphere-2025-4446
Preprint. Discussion started: 18 September 2025

N_2O fluxes showed strong seasonal patterns: predominantly positive in spring (0.003 to 0.02 mg N_2O m^{-2} d^{-1}) and negative in fall (-0.02 to -0.003 mg N_2O m^{-2} d^{-1}). This seasonal switch from source to sink behavior is consistent with findings by Brunberg et al. (2025) and Cheung et al. (2025), who reported similar patterns in Eastern and Southern coastal Baltic areas.

Our estimated flux densities are generally at the lower end of values reported from previous studies in the Baltic Sea, Swedish lakes, and global estimates for other coastal habitats (see table 5). The more moderate fluxes observed in our study sites likely reflect the sheltered nature of these shallow bays and the relatively low wind speeds we encountered during our measurements.

Table 5. Range and median values (if available) of flux densities reported from different coastal habitats.

Study	F_{CO_2} (mg CO_2 m^{-2} d^{-1})	F_{CH_4} (mg CH_4 m^{-2} d^{-1})	F_{N_2O} (mg N_2O m^{-2} d^{-1})	Location
		Western Baltic Sea		
This study	-68–303 (27.5)	0.05–1.1 (0.48)	-0.02–0.02 (-0.005)	Stockholm Archipelago
Lundevall-Zara et al. (2021)	-	0.3–162	-	Askö
Roth et al. (2022)	-	0.05-0.69 (0.19)	-	Askö, mixed vegetated
	-	0.03-0.51 (0.16)	-	Askö, algae-dominated
	-	0.03-0.465 (0.11)	-	Askö, bare sediments
		Eastern Baltic Sea		
Brunberg et al.	-1798 – 1112 (-72)	-0.17–2.5 (0.3)	-0.04–0.48 (0.08)	Tvärminne Archipelago
Asmala and Scheinin (2024)	-7000–-108000 (180±4000)	-0.9–478 (31.0±50.0)	-	Tvärminne Archipelago
Humborg et al. (2019)	3300–12000	-	-	Tvärminne Archipelago
		Southern Baltic Sea		
Cheung et al. (2025)	-	-	-0.07-–0.48 (0.19)	Curonian lagoon
	-	-	-0.04-–0.25 (0.11)	Oder lagoon
	-	-	-0.02—0.19 (0.09)	Vistula lagoon
Bange et al. (1998)	-	0.82–5.9	0.02-0.31	Bodden waters
Bange et al. (2010)	-	0.1–0.23	-	Boknis Eck
Ma et al. (2019)	-	-	-0.6–1.33	Boknis Eck
Ma et al. (2020)	-	0.005–11.97	-	Boknis Eck
Heyer and Berger (2000)	-	2.4–2496	-	Rügen
		Swedish lakes		
Bastviken et al. (2004)	-	0.19–4.2	-	
Humborg et al. (2010)	320–883.6	-	-	
		Global		
Rosentreter et al. (2023)	1020–1490 (1220)	0.67–0.85 (0.77)	0.20–0.29 (0.25)	Tidal systems
	570–950 (710)	0.77–1.54 (1.32)	0.09–0.20 (0.15)	Lagoons
	-610–100 (-340)	0.03–0.06 (0.04)	0.23–0.22 (0.17)	Fjords
	-8310– -6780 (-7250)	4.64–7.51 (6.11)	0.05–0.23 (0.13)	Mangroves
	-2700– -2090 (-2130)	6.23–15.36 (10.57)	0.01–0.20 (0.11)	Salt marshes
	-2960– -500 (-1630)	1.20–1.63 (1.47)	-0.05– -0.3 (-0.04)	Sea grasses

https://doi.org/10.5194/egusphere-2025-4446
Preprint. Discussion started: 18 September 2025

3.3 CO_2-equivalent fluxes and net greenhouse gas balance

To asses the overall climate impact, individual gas fluxes were converted to CO_2-equivalent fluxes using 100-year sustained global warming potentials of 45 for CH_4 and 270 for N_2O. Total net CO_2-equivalent fluxes, varied significantly between bays and seasons, ranging from -76.1 mg CO_2-eq m^{-2} d^{-1} (net sink) in Assöviken in Spring to 710.8 mg CO_2-eq m^{-2} d^{-1} (net source) in Östra Lermaren in fall, with a median of 56.9 mg CO_2-eq m^{-2} d^{-1} across all measurements.

Most bays acted as net greenhouse gas sources, with only Sandviken and Assöviken showing net sink behavior in April. CO_2 fluxes generally dominated the greenhouse gas balance. However, in Högklykeviken, CH_4 emissions nearly balanced CO_2 uptake in spring and even exceeded CO_2 influx in fall (see Fig. 4 and Table A4 in the appendix) highlighting the potential importance of CH_4 in degraded coastal systems. N_2O contributions were generally minor, except in Sandviken in April, where N_2O efflux accounted for 15% of the net flux. The large variability observed across bays and seasons underscores the challenge of scaling up fluxes from such heterogeneous environments. Nevertheless, to provide rough estimates of regional contributions, we multiplied our total CO_2-equivalent fluxes by the estimated total area of shallow, enclosed bays in the archipelagos around Stockholm, Uppsala, Åland and southwestern Finland (142 km^2, Gubri et al., 2025). This calculation results in total carbon fluxes ranging from -2.95 t C d^{-1} to 27.5 t C d^{-1} with a median of 2.2 t C d^{-1}. These estimates highlight both the potential regional significance of these shallow bay systems and the enormous uncertainty when extrapolating from limited spatial and temporal measurements. The wide range emphasizes the need for more comprehensive monitoring to better constrain regional greenhouse gas budgets from coastal ecosystems.

https://doi.org/10.5194/egusphere-2025-4446
Preprint. Discussion started: 18 September 2025

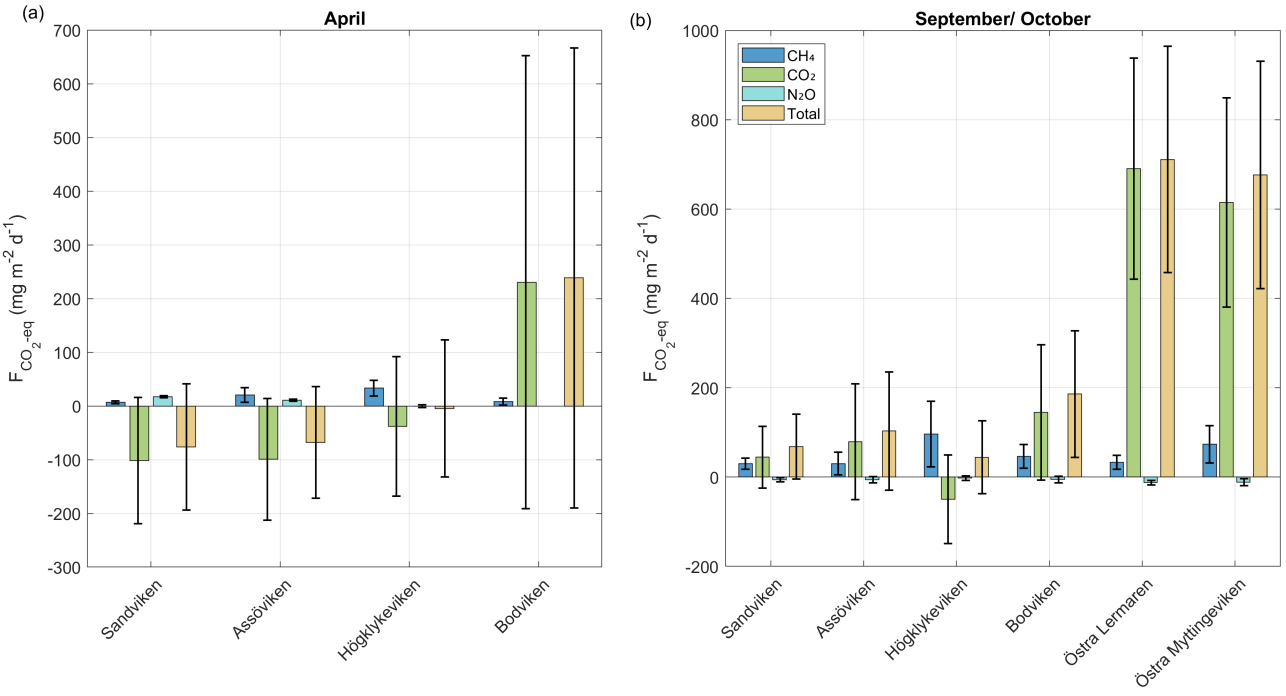

Figure 4. CO_2 equivalent fluxes of CH_4, CO_2, N_2O and total fluxes from all bays in (a) April and (b) September/October estimated based on the parameterization by Cole and Caraco (1998). Bars represent mean values and the error bars represent the standard deviation.

4 Conclusions

This study provides a comprehensive assessment of GHG emissions (CO_2, CH_4 and N_2O) from shallow coastal bays in the Baltic Sea, and is one of the few investigations to simultaneously measure all three major GHGs across multiple bay environments. The results highlight the complex and highly variable nature of GHG dynamics in these systems. Our findings demonstrate that shallow Baltic Sea bays are significant but highly variable sources of GHGs, with net CO_2-equivalent fluxes ranging from -76.1 mg CO_2-eq m^{-2} d^{-1} in Spring to 710.8 mg CO_2-eq m^{-2} d^{-1} in fall (median 56.9 mg CO_2-eq m^{-2} d^{-1} across all bays and seasons). Each GHG showed different behavior with differing spatial and temporal variability: CO_2 has the highest variability and generally dominated fluxes, CH_4 was routinely elevated inside the bays and increased from spring to fall, while N_2O showed opposite seasonal trends with higher concentrations outside the bays.

Interestingly, we observed a threshold behavior in N_2O-CH_4 correlations. In the two bays with the highest concentrations of CH_4, we observed a shift from negative correlations at CH_4 levels below 250 nmol L^{-1} to positive correlations above this threshold. This is a pattern that has not previously been reported in coastal environments.

By contextualizing GHG fluxes within a broader environmental framework, this study provides important observational insights into the potential environmental controls on coastal GHG dynamics. Bay characteristics, including openness, eutroph-

https://doi.org/10.5194/egusphere-2025-4446
Preprint. Discussion started: 18 September 2025

ication status, sediment properties, and vegetation cover, influenced gas concentrations and fluxes, although the high spatial and temporal variability complicated statistical analysis with our limited number of study sites.

The substantial variability observed between bays and seasons underscores both the complexity of these systems and the challenges in scaling up coastal GHG estimates. However, our findings suggest that shallow enclosed bays may represent an overlooked but important component of coastal GHG budgets.

This study represents temporal and spatial snapshots that compare four to six bays in two seasons. Scaling up from such limited measurements risks substantial under- or overestimation of coastal ecosystems contributions to global GHG budgets. Given this, future research should prioritize two key areas. Firstly, long-term monitoring combining eddy-covariance flux measurements with seawater monitoring would better capture annual and interannual variability while identifying the biological drivers of emissions, particularly methanogenic and methanotrophic communities. Secondly, research is needed to differentiate between ebullitive and diffusive CH_4 fluxes and to analyze factors that promote ebullition across seasonal timescales.

The increasing frequency of seasonal anoxia in coastal areas of the Baltic Sea, driven by eutrophication and climate change, will likely intensify GHG emissions from coastal areas. As such, understanding these dynamics is becoming increasingly important as coastal development and nutrient pollution continue to impact these systems.

Future research is needed to develop management frameworks that consider GHG emissions alongside traditional water quality concerns. Finally, this research provides important baseline data and methodological approaches for future investigations of GHG dynamics in shallow coastal ecosystems, and importantly, the results contribute to a more accurate scaling of coastal GHG emissions and highlight the importance of including these systems in regional and global GHG budgets.

Data availability. Data will be made available prior to publication.

Author contributions. The study was conceptualized jointly by all authors (JH, SW, LK, ER, CH, JZ, MH, AF, MS). JZ performed the water column GHG measurements (with help from CH and MS) and AF and MH collected and processed the sediment cores (with assistance from all other co-authors). JZ carried out the data analysis and visualization, and prepared the initial manuscript draft, with input from all co-authors. JH provided vegetation and seawater property data, and MH contributed the sediment data. MG developed the WEGAS system and trained JZ in its use.

Competing interests. The authors declare no competing interests.

https://doi.org/10.5194/egusphere-2025-4446
Preprint. Discussion started: 18 September 2025

Acknowledgements. We gratefully acknowledge the financial support provided by the BalticWaters foundation (project “Thriving Bays”). The study is conducted in collaboration with the Centre for Coastal Ecosystem and Climate Change Research (www.coastclim.org). We extend our thanks to Ulf Lindqvist and Maria Arvidsson (Naturvatten in Roslagen AB) for assistance in the field and Prof. Johan S. Eklöf (Department of Ecology, Environment and Plant Sciences, Stockholm University) for sharing vegetation data from one of the bays.

https://doi.org/10.5194/egusphere-2025-4446
Preprint. Discussion started: 18 September 2025

Appendix A

A1 Tables

Table A1. A Kruskal-Wallis test was conducted on 10% of the data in each bay to test whether the concentrations of GHGs inside the different bays were significantly different. A difference is significant if $p < 0.01$.

	April	September/ October
CO_2	$p = 0.007$	$p = 3.3e^{-24}$
CH_4	$p = 4.9e^{-29}$	$p = 1.78e^{-11}$
N_2O	$p = 1.3e^{-46}$	$p = 5.4e^{-5}$

Table A2. Bonferroni-adjusted p-values from post hoc pairwise comparisons between bays; values less than 0.05 indicate statistically significant differences. No data is available for Östra Lermaren (ÖL) and Östra Myttingeviken (ÖM) in April. Furthermore, no N_2O data is available for Bodenviken (BV) in April.

		April			September/October		
Group A	Group B	p_{CO_2}	p_{CH_4}	p_{N_2O}	p_{CO_2}	p_{CH_4}	p_{N_2O}
SV	AV	1	$4.8e^{-8}$	$2.9e^{-23}$	1	1	1
SV	HV	0.014	$1.1e^{-24}$	$4.1e^{-31}$	0.46	0.0025	0.003
SV	BV	0.58	1	-	1	0.217	1
SV	ÖL	-	-	-	$3.7e^{-8}$	1	1
SV	ÖM	-	-	-	$2.24e^{-9}$	$1.07e^{-7}$	0.915
AV	HV	0.046	0.001	0.35	0.197	$1.55e^{-4}$	$6.75e^{-5}$
AV	BV	0.62	$1.38e^{-5}$	-	1	0.035	0.24
AV	ÖL	-	-	-	$2.98e^{-8}$	1	1
AV	ÖM	-	-	-	$1.86e^{-9}$	$1.8e^{-9}$	0.15
HV	BV	1	$1.5e^{-15}$	-	0.02	1	0.49
HV	ÖL	-	-	-	$4.56e^{-15}$	0.033	0.007
HV	ÖM	-	-	-	$4.74e^{-16}$	0.27	1
BV	ÖL	-	-	-	$5.14e^{-6}$	1	1
BV	ÖM	-	-	-	$3.08e^{-7}$	0.004	1
ÖL	ÖM	-	-	-	1	$4.04e^{-6}$	1

https://doi.org/10.5194/egusphere-2025-4446
Preprint. Discussion started: 18 September 2025

Table A3. A Wilcoxon ranksum test was conducted to test whether the concentrations of GHGs inside and outside the bays were significantly different. A difference is significant if $h = 1$ and $p < 0.05$. No data is available outside Östra Myttingeviken and no N_2O data is available for Bodviken (BV).

	April				September/October				
	SV	AV	HV	BV	SV	AV	HV	BV	ÖL
CO_2	$h = 1$ $p = 6e^{-183}$	$h = 1$ $p = 4.1e^{-57}$	$h = 1$ $p = 5.1e^{-68}$	$h = 1$ $p = 1.2e^{-58}$	$h = 1$ $p = 5.9e^{-20}$	$h = 1$ $p = 2.15e^{-37}$	$h = 1$ $p = 6.85e^{-16}$	$h = 1$ $p = 1e^{-38}$	$h = 1$ $p = 9.8e^{-29}$
CH_4	$h = 1$ $p = 9.3e^{-70}$	$h = 1$ $p = 1.6e^{-8}$	$h = 1$ $p = 7.85e^{-47}$	$h = 1$ $p = 1.2e^{-58}$	$h = 1$ $p = 7e^{-61}$	$h = 1$ $p = 5.9e^{-34}$	$h = 1$ $p = 1.1e^{-46}$	$h = 1$ $p = 1.65e^{-52}$	$h = 1$ $p = 7.5e^{-29}$
N_2O	$h = 1$ $p = 8.7e^{-79}$	$h = 1$ $p = 1.7e^{-66}$	$h = 1$ $p = 3.4e^{-62}$	NA NA	$h = 1$ $p = 2.2e^{-36}$	$h = 1$ $p = 4.6e^{-36}$	$h = 1$ $p = 1.65e^{-43}$	$h = 1$ $p = 1.8e^{-52}$	$h = 1$ $p = 7.7e^{-29}$

Table A4. Percentage contribution to the total net flux calculated as $\frac{\text{abs(mean}(F_{X,CO_2-eq}))}{\text{abs(mean}(F_{CO_2}))+\text{abs(mean}(F_{CH_4,CO_2-eq}))+\text{abs(mean}(F_{N_2O,CO_2-eq}))}$. No N_2O data is available for Bodviken in April.

	April				September/October					
	SV	AV	HV	BV	SV	AV	HV	BV	ÖL	ÖM
CO_2	80%	76%	53.2%	96.5%	55.4%	68.5%	33.5%	73.7%	93.8%	87.8%
CH_4	5%	15.6%	46.2%	3.5%	37.2%	26.3%	65%	23.5%	4.5%	10.5%
N_2O	15%	8.4%	0.5%	-	7.5%	5.3%	1.5%	2.8%	1.7%	1.7%

https://doi.org/10.5194/egusphere-2025-4446
Preprint. Discussion started: 18 September 2025

A2 Figures

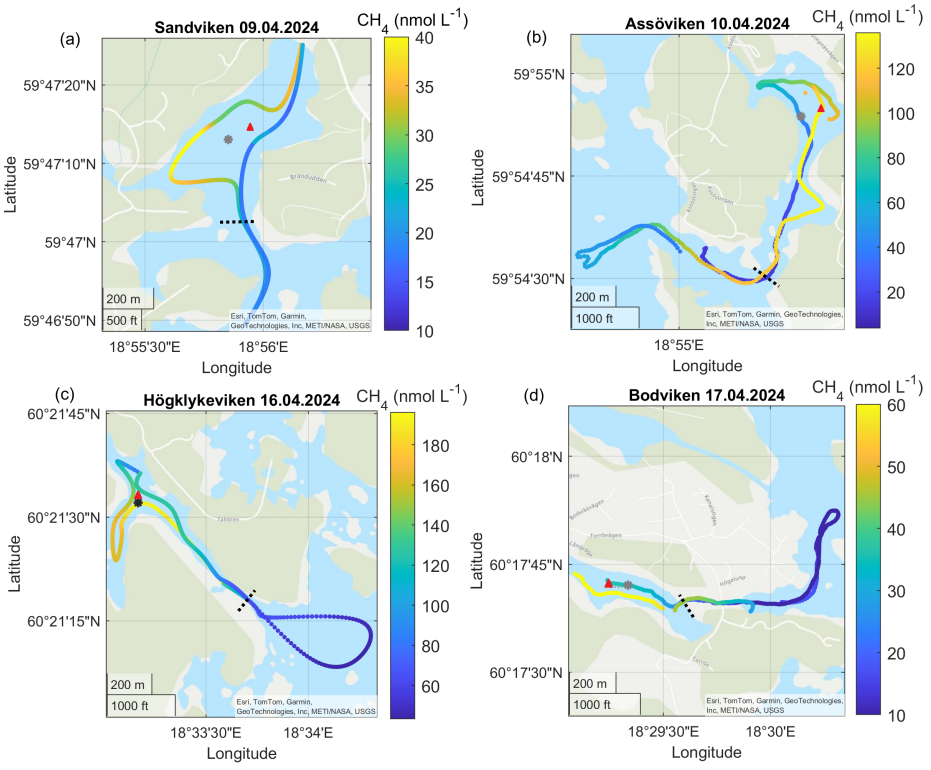

Figure A1. Surface water CH_4 concentrations in the different bays in April. Note the differences in scale between the different panels. The gray dots marks the sediment/water sampling locations during the GHG measurements, while red triangles mark long-term water monitoring stations. The dashed line marks the division between inside and outside bay area.

https://doi.org/10.5194/egusphere-2025-4446
Preprint. Discussion started: 18 September 2025

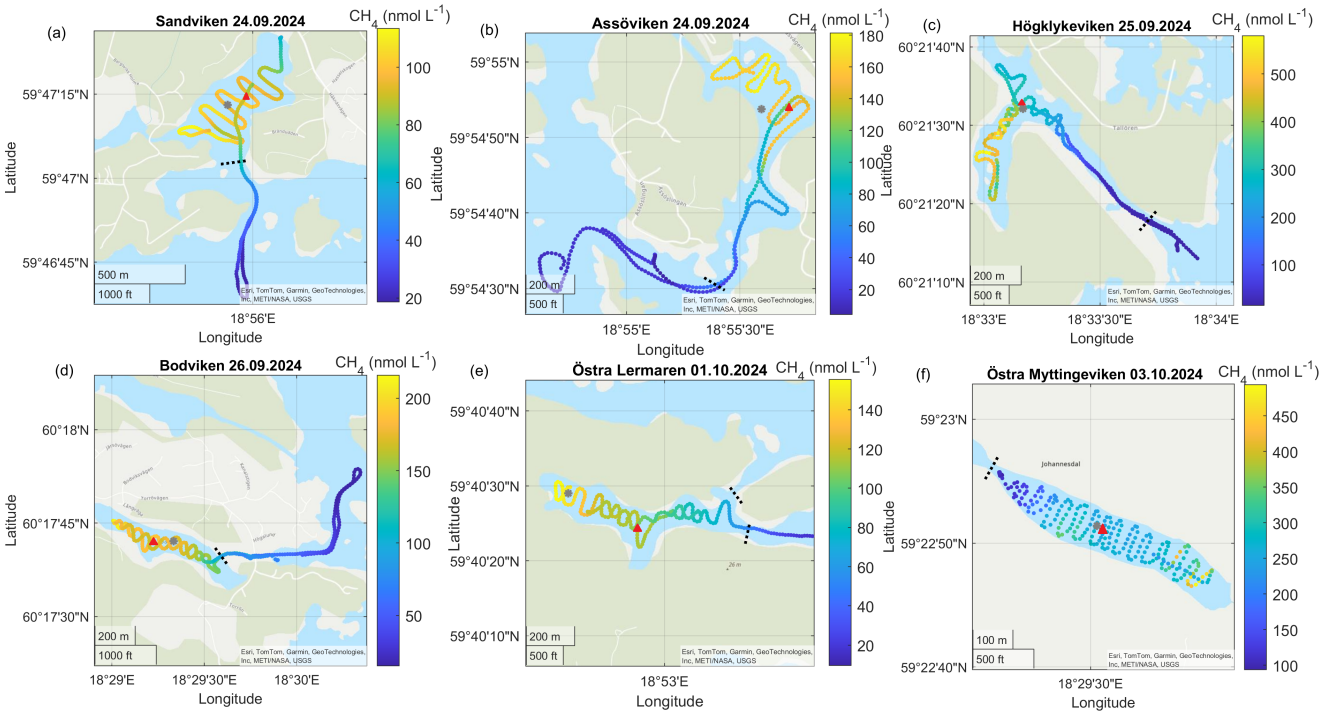

Figure A2. Surface water CH_4 concentrations in the different bays in September - October. Note the differences in scale between the different panels. The gray dots marks the sediment/water sampling locations during the GHG measurements, while red triangles mark long-term water monitoring stations. The dashed line marks the division between inside and outside bay area.

https://doi.org/10.5194/egusphere-2025-4446
Preprint. Discussion started: 18 September 2025

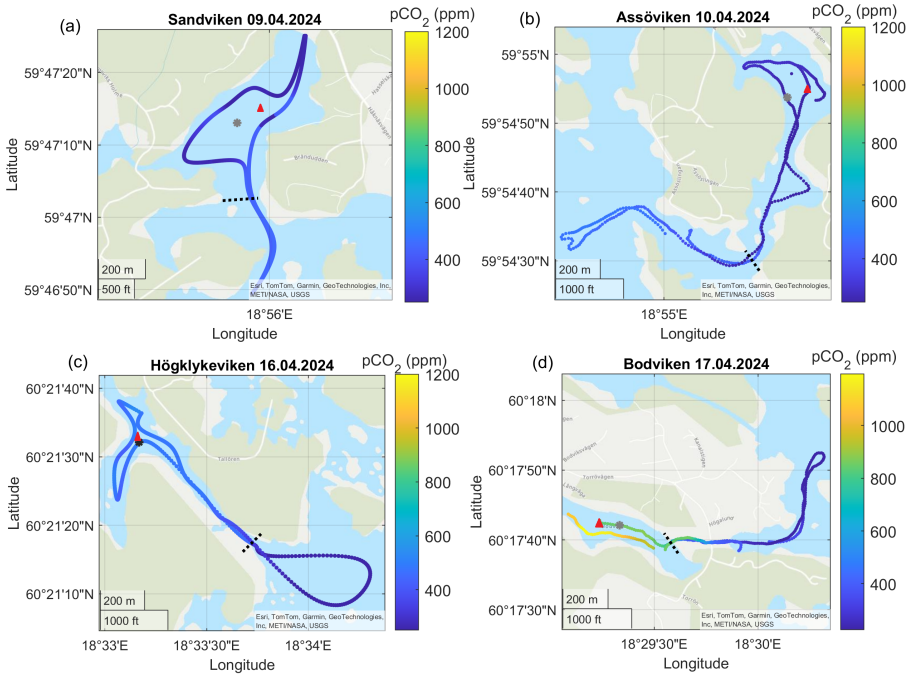

Figure A3. Surface water pCO_2 concentrations in the different bays in April. The gray dots marks the sediment/water sampling locations during the GHG measurements, while red triangles mark long-term water monitoring stations. The dashed line marks the division between inside and outside bay area.

https://doi.org/10.5194/egusphere-2025-4446
Preprint. Discussion started: 18 September 2025

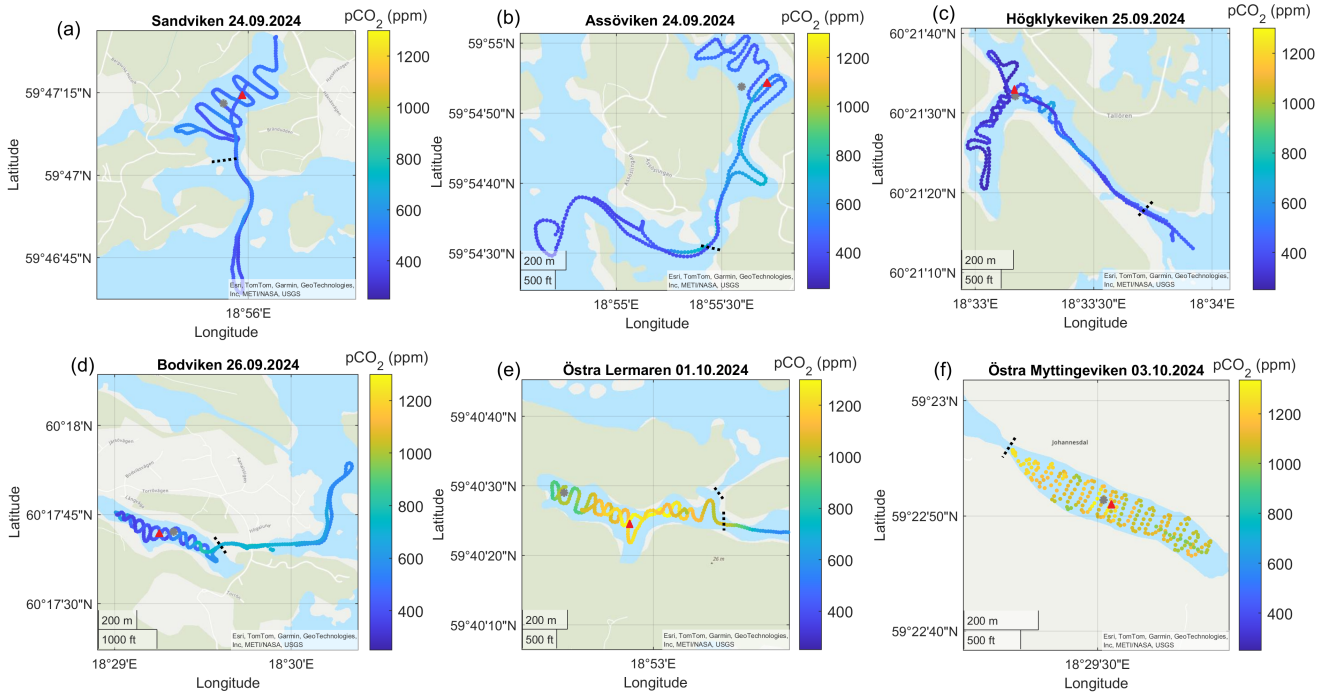

Figure A4. Surface water pCO_2 concentrations in the different bays in September - October. The gray dots marks the sediment/water sampling locations during the GHG measurements, while red triangles mark long-term water monitoring stations. The dashed line marks the division between inside and outside bay area.

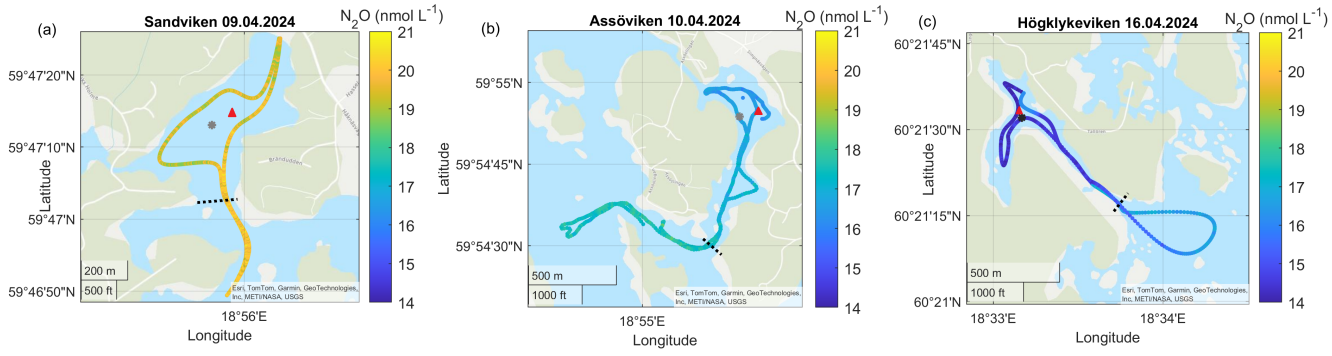

Figure A5. Surface water N_2O concentrations in the different bays in April. No N_2O data is available for Bodviken. The gray dots marks the sediment/water sampling locations during the GHG measurements, while red triangles mark long-term water monitoring stations. The dashed line marks the division between inside and outside bay area.

https://doi.org/10.5194/egusphere-2025-4446
Preprint. Discussion started: 18 September 2025

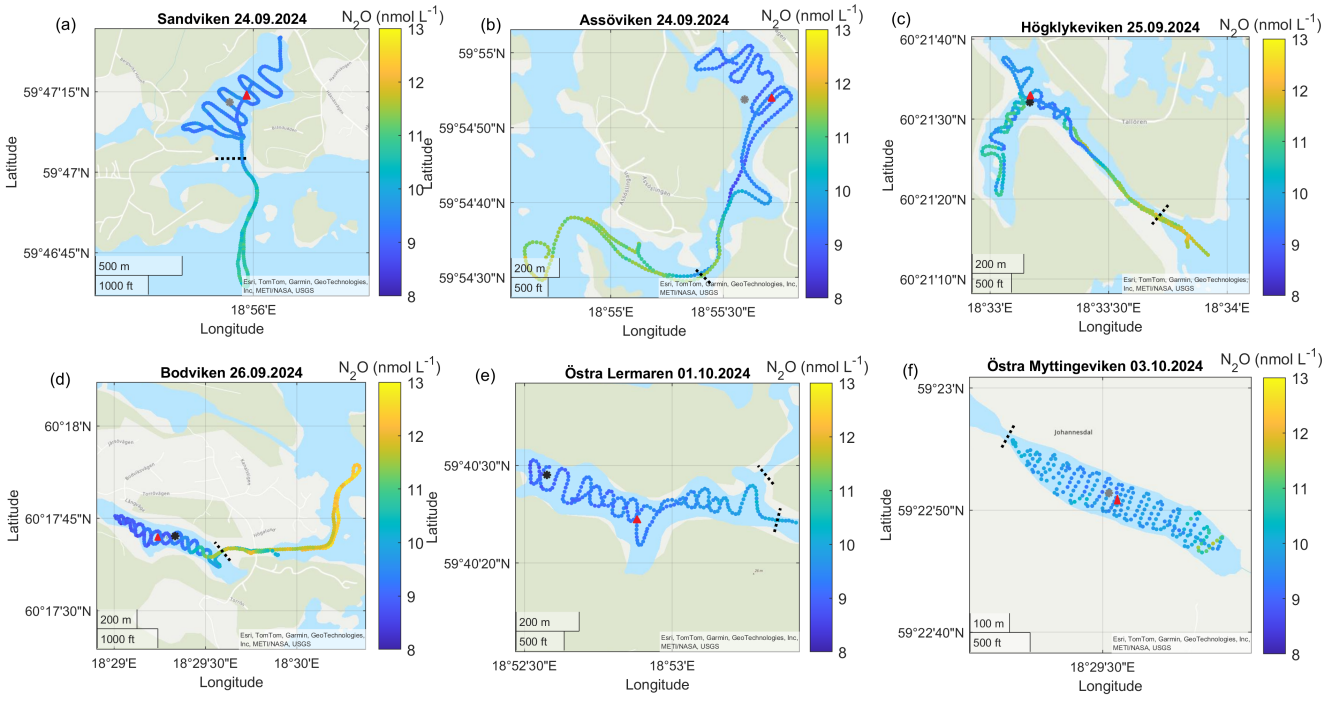

Figure A6. Surface water N_2O concentrations in the different bays in September - October. The gray dots marks the sediment/water sampling locations during the GHG measurements, while red triangles mark long-term water monitoring stations. The dashed line marks the division between inside and outside bay area.

https://doi.org/10.5194/egusphere-2025-4446
Preprint. Discussion started: 18 September 2025

References

Al-Haj, A. N. and Fulweiler, R. W.: A synthesis of methane emissions from shallow vegetated coastal ecosystems, Global Change Biology, 26, 2988–3005, 2020.

Amaral, V., Ortega, T., Romera-Castillo, C., and Forja, J.: Linkages between greenhouse gases (CO_2, CH_4, and N_2O) and dissolved organic matter composition in a shallow estuary, Science of the Total Environment, 788, 147 863, 2021.

Asmala, E. and Scheinin, M.: Persistent hot spots of CO_2 and CH_4 in coastal nearshore environments, Limnology and Oceanography Letters, 9, 119–127, 2024.

Bange, H. W., Dahlke, S., Ramesh, R., Meyer-Reil, L.-A., Rapsomanikis, S., and Andreae, M.: Seasonal study of methane and nitrous oxide in the coastal waters of the southern Baltic Sea, Estuarine, Coastal and Shelf Science, 47, 807–817, 1998.

Bange, H. W., Bergmann, K., Hansen, H. P., Kock, A., Koppe, R., Malien, F., and Ostrau, C.: Dissolved methane during hypoxic events at the Boknis Eck time series station (Eckernförde Bay, SW Baltic Sea), Biogeosciences, 7, 1279–1284, 2010.

Barnes, J. and Upstill-Goddard, R. C.: The denitrification paradox: The role of O_2 in sediment N_2O production, Estuarine, Coastal and Shelf Science, 200, 270–276, 2018.

Bastviken, D., Cole, J., Pace, M., and Tranvik, L.: Methane emissions from lakes: Dependence of lake characteristics, two regional assessments, and a global estimate, Global biogeochemical cycles, 18, 2004.

Brunberg, M., Roth, F., Geibel, M. C., Gustafsson, E., Vähä, A., Norkko, A., and Humborg, C.: Hot spots and hot moments in greenhouse gas (CO_2, CH_4 and N_2O) fluxes in a diverse coastal ecosystem, under review at Limnology & Oceanography Research Letters, 2025.

Burdige, D. J.: Geochemistry of marine sediments, 2020.

Camacho, A., Picazo, A., Rochera, C., Santamans, A. C., Morant, D., Miralles-Lorenzo, J., and Castillo-Escriva, A.: Methane emissions in Spanish saline lakes: current rates, temperature and salinity responses, and evolution under different climate change scenarios, Water, 9, 659, 2017.

Cheung, H. L., Zilius, M., Politi, T., Lorre, E., Vybernaite-Lubiene, I., Santos, I. R., and Bonaglia, S.: Nitrate-driven eutrophication supports high nitrous oxide production and emission in coastal lagoons, Journal of Geophysical Research: Biogeosciences, 130, e2024JG008 510, 2025.

Codispoti, L. A.: Interesting times for marine N_2O, Science, 327, 1339–1340, 2010.

Cole, J. J. and Caraco, N. F.: Atmospheric exchange of carbon dioxide in a low-wind oligotrophic lake measured by the addition of SF6, Limnology and Oceanography, 43, 647–656, 1998.

Conrad, R.: The global methane cycle: recent advances in understanding the microbial processes involved, Environmental microbiology reports, 1, 285–292, 2009.

Denman, K. L., Brasseur, G., Chidthaisong, A., Ciais, P., Cox, P. M., Dickinson, R. E., Hauglustaine, D., Heinze, C., Holland, E., Jacob, D., et al.: Couplings between changes in the climate system and biogeochemistry, Climate Change 2007: The Physical Science Basis. Contribution of Working Group I to the Fourth Assessment Report of the Intergovernmental Panel on Climate Change The Physical Science Basis, pp. 499–587, 2007.

Elkins, J. W., Wofsy, S. C., McElroy, M. B., Kolb, C. E., and Kaplan, W. A.: Aquatic sources and sinks for nitrous oxide, Nature, 275, 602–606, 1978.

Foster, S. Q. and Fulweiler, R. W.: Sediment nitrous oxide fluxes are dominated by uptake in a temperate estuary, Frontiers in Marine Science, 3, 40, 2016.

https://doi.org/10.5194/egusphere-2025-4446
Preprint. Discussion started: 18 September 2025

Gubri, B., Hansen, J. P., Wikström, S. A., Snickars, M., Dahl, M., Gullström, M., Rydin, E., Masqué, P., Garbaras, A., Björk, M., et al.: Shallow Coastal Bays as Sediment Carbon and Nutrient Reservoirs in the Baltic Sea, Estuaries and Coasts, 48, 1–16, 2025.

Hansen, J. P., Wikström, S. A., and Kautsky, L.: Effects of water exchange and vegetation on the macroinvertebrate fauna composition of shallow land-uplift bays in the Baltic Sea, Estuarine, Coastal and Shelf Science, 77, 535–547, 2008.

Hermans, M., Stranne, C., Broman, E., Sokolov, A., Roth, F., Nascimento, F. J., Mörth, C.-M., Ten Hietbrink, S., Sun, X., Gustafsson, E., et al.: Ebullition dominates methane emissions in stratified coastal waters, Science of the Total Environment, 945, 174 183, 2024.

Heyer, J. and Berger, U.: Methane emission from the coastal area in the southern Baltic Sea, Estuarine, Coastal and Shelf Science, 51, 13–30, 2000.

Humborg, C., Mörth, C.-M., Sundbom, M., Borg, H., Blenckner, T., Giesler, R., and Ittekkot, V.: CO_2 supersaturation along the aquatic conduit in Swedish watersheds as constrained by terrestrial respiration, aquatic respiration and weathering, Global Change Biology, 16, 1966–1978, 2010.

Humborg, C., Geibel, M. C., Sun, X., McCrackin, M., Mörth, C.-M., Stranne, C., Jakobsson, M., Gustafsson, B., Sokolov, A., Norkko, A., et al.: High emissions of carbon dioxide and methane from the coastal Baltic Sea at the end of a summer heat wave, Frontiers in Marine Science, 6, 493, 2019.

Ji, Q., Babbin, A. R., Jayakumar, A., Oleynik, S., and Ward, B. B.: Nitrous oxide production by nitrification and denitrification in the Eastern Tropical South Pacific oxygen minimum zone, Geophysical Research Letters, 42, 10–755, 2015.

Ji, Q., Buitenhuis, E., Suntharalingam, P., Sarmiento, J. L., and Ward, B. B.: Global nitrous oxide production determined by oxygen sensitivity of nitrification and denitrification, Global Biogeochemical Cycles, 32, 1790–1802, 2018.

Lundevall-Zara, M., Lundevall-Zara, E., and Brüchert, V.: Sea-air exchange of methane in shallow inshore areas of the Baltic Sea, Frontiers in Marine Science, 8, 657 459, 2021.

Ma, X., Lennartz, S. T., and Bange, H. W.: A multi-year observation of nitrous oxide at the Boknis Eck Time Series Station in the Eckernförde Bay (southwestern Baltic Sea), Biogeosciences, 16, 4097–4111, 2019.

Ma, X., Sun, M., Lennartz, S. T., and Bange, H. W.: A decade of methane measurements at the Boknis Eck time series station in Eckernförde Bay (southwestern Baltic Sea), Biogeosciences, 17, 3427–3438, 2020.

Munsterhjelm, R.: The aquatic macrophyte vegetation of flads and gloes, S coast of Finland, Acta Bot. Fenn., p. 68, 1997.

Murray, R. H., Erler, D. V., and Eyre, B. D.: Nitrous oxide fluxes in estuarine environments: response to global change, Global change biology, 21, 3219–3245, 2015.

Myllykangas, J.-P., Hietanen, S., and Jilbert, T.: Legacy effects of eutrophication on modern methane dynamics in a boreal estuary, Estuaries and Coasts, 43, 189–206, 2020.

Naqvi, S., Bange, H. W., Farías, L., Monteiro, P., Scranton, M., and Zhang, J.: Marine hypoxia/anoxia as a source of CH_4 and N_2O, Biogeosciences, 7, 2159–2190, 2010.

Neubauer, S. C. and Megonigal, J. P.: Moving beyond global warming potentials to quantify the climatic role of ecosystems, Ecosystems, 18, 1000–1013, 2015.

Persson, J., Håkanson, L., and Pilesjö, P.: Prediction of surface water turnover time in coastal waters using digital bathymetric information, Environmetrics, 5, 433–449, 1994.

Poffenbarger, H. J., Needelman, B. A., and Megonigal, J. P.: Salinity influence on methane emissions from tidal marshes, Wetlands, 31, 831–842, 2011.

https://doi.org/10.5194/egusphere-2025-4446
Preprint. Discussion started: 18 September 2025

Reay, D. S., Smith, P., Christensen, T. R., James, R. H., and Clark, H.: Methane and global environmental change, Annual Review of Environment and Resources, 43, 165–192, 2018.

Reeburgh, W. S.: Oceanic methane biogeochemistry, Chemical reviews, 107, 486–513, 2007.

Reitzel, K., Ahlgren, J., Gogoll, A., and Rydin, E.: Effects of aluminum treatment on phosphorus, carbon, and nitrogen distribution in lake sediment: a 31P NMR study, Water research, 40, 647–654, 2006.

Resplandy, L., Hogikyan, A., Müller, J. D., Najjar, R. G., Bange, H. W., Bianchi, D., Weber, T., Cai, W.-J., Doney, S. C., Fennel, K., et al.: A synthesis of global coastal ocean greenhouse gas fluxes, Global Biogeochemical Cycles, 38, e2023GB007 803, 2024.

Rosentreter, J. A., Al-Haj, A. N., Fulweiler, R. W., and Williamson, P.: Methane and nitrous oxide emissions complicate coastal blue carbon assessments, Global Biogeochemical Cycles, 35, e2020GB006 858, 2021a.

Rosentreter, J. A., Borges, A. V., Deemer, B. R., Holgerson, M. A., Liu, S., Song, C., Melack, J., Raymond, P. A., Duarte, C. M., Allen, G. H., et al.: Half of global methane emissions come from highly variable aquatic ecosystem sources, Nature Geoscience, 14, 225–230, 2021b.

Rosentreter, J. A., Laruelle, G. G., Bange, H. W., Bianchi, T. S., Busecke, J. J., Cai, W.-J., Eyre, B. D., Forbrich, I., Kwon, E. Y., Maavara, T., et al.: Coastal vegetation and estuaries are collectively a greenhouse gas sink, Nature Climate Change, 13, 579–587, 2023.

Roth, F., Sun, X., Geibel, M. C., Prytherch, J., Brüchert, V., Bonaglia, S., Broman, E., Nascimento, F., Norkko, A., and Humborg, C.: High spatiotemporal variability of methane concentrations challenges estimates of emissions across vegetated coastal ecosystems, Global change biology, 28, 4308–4322, 2022.

Sander, R.: Compilation of Henry's law constants (version 4.0) for water as solvent, Atmospheric Chemistry and Physics, 15, 4399–4981, 2015.

Scalize, P., Albuquerque, A., and Di Bernardo, L.: Impact of alum water treatment residues on the methanogenic activity in the digestion of primary domestic wastewater sludge, Sustainability, 13, 8783, 2021.

Scheinin, M. and Mattila, J.: The structure and dynamics of zooplankton communities in shallow bays in the northern Baltic Sea during a single growing season, Boreal Environment Research, 15, 397, 2010.

Schubert, C. J. and Wehrli, B.: Contribution of methane formation and methane oxidation to methane emission from freshwater systems, in: Biogenesis of hydrocarbons, pp. 401–430, Springer, 2019.

Snickars, M., Sandström, A., Lappalainen, A., Mattila, J., Rosqvist, K., and Urho, L.: Fish assemblages in coastal lagoons in land-uplift succession: the relative importance of local and regional environmental gradients, Estuarine, Coastal and Shelf Science, 81, 247–256, 2009.

Stein, L. Y.: The long-term relationship between microbial metabolism and greenhouse gases, Trends in microbiology, 28, 500–511, 2020.

Tang, W., Tracey, J. C., Carroll, J., Wallace, E., Lee, J. A., Nathan, L., Sun, X., Jayakumar, A., and Ward, B. B.: Nitrous oxide production in the Chesapeake Bay, Limnology and Oceanography, 67, 2101–2116, 2022.

Venetz, J., Żygadłowska, O. M., Dotsios, N., Wallenius, A. J., van Helmond, N. A., Lenstra, W. K., Klomp, R., Slomp, C. P., Jetten, M. S., and Veraart, A. J.: Seasonal dynamics of the microbial methane filter in the water column of a eutrophic coastal basin, FEMS Microbiology Ecology, 100, fiae007, 2024.

Wanninkhof, R.: Relationship between wind speed and gas exchange over the ocean revisited, Limnology and Oceanography: Methods, 12, 351–362, 2014.

Weber, T., Wiseman, N. A., and Kock, A.: Global ocean methane emissions dominated by shallow coastal waters, Nature communications, 10, 4584, 2019.

https://doi.org/10.5194/egusphere-2025-4446
Preprint. Discussion started: 18 September 2025

Wiesenburg, D. A. and Guinasso Jr, N. L.: Equilibrium solubilities of methane, carbon monoxide, and hydrogen in water and sea water, Journal of chemical and engineering data, 24, 356–360, 1979.

Wikström, S. A., Gubri, B., Asplund, M. E., Dahl, M., Gullström, M., Hansen, J. P., Kumblad, L., Rydin, E., Garbaras, A., and Björk, M.: Influence of landscape characteristics and submerged aquatic vegetation on sediment carbon and nitrogen storage in shallow brackish water habitats, Scientific Reports, 15, 7808, 2025.

Yvon-Durocher, G., Allen, A. P., Bastviken, D., Conrad, R., Gudasz, C., St-Pierre, A., Thanh-Duc, N., and Del Giorgio, P. A.: Methane fluxes show consistent temperature dependence across microbial to ecosystem scales, Nature, 507, 488–491, 2014.

Zhou, L., Tan, Y., Huang, L., Fortin, C., and Campbell, P. G.: Aluminum effects on marine phytoplankton: implications for a revised iron hypothesis (iron–aluminum hypothesis), Biogeochemistry, 139, 123–137, 2018.

Żygadłowska, O. M., Venetz, J., Klomp, R., Lenstra, W. K., van Helmond, N. A., Röckmann, T., Wallenius, A. J., Martins, P. D., Veraart, A. J., Jetten, M. S., et al.: Pathways of methane removal in the sediment and water column of a seasonally anoxic eutrophic marine basin, Frontiers in Marine Science, 10, 1085 728, 2023.